

Using fluorescently labelled aCD47, fibrinogen and nanoparticles, the authors tracked each gel component over time, confirming uniform distribution and gradual release of aCD47 into the tissue and complete biodegradation of the gel after three weeks. Application of the aCD47-loaded gel to wounds of tumour-resected mice led to induction of both the innate and adaptive immune system at the surgical site, enhanced destruction of cancer cells, decreased tumour regrowth, and ultimately a significant increase in survival, without induction of significant side effects. Additionally, Chen et al. showed that if the tumour resection cavity was spray-treated, tumour growth was also decreased at distant sites, inhibiting metastases. In fact, the immunotherapeutic spray seems to activate the adaptive and innate immune system not only locally but also systemically: that is, throughout the entire organism. The local as well as systemic effects were further improved by using a combination of aCD47 plus a T-cell-activating antibody (anti-PD-1).

This paper is of relevance for the field of oncology, especially considering the spray's apparent low toxicity and ease of application. As the authors acknowledge, assuring clinical translation, with a maximum of desired effects at a minimum of unwanted side effects, will require validation of the results in larger animal models and larger cohorts, which will also help in further defining the precise modalities of application. This includes, for example, determining dose levels and optimizing the release kinetics of the immune-active substances, ultimately aiming at improving outcomes such as overall survival, disease-free survival or progression-free survival. As CD47 inhibitors have been shown to have side effects such as anaemia and thrombocytopenia in systemic administration in clinical trials, it remains to be understood whether a local application might reduce such toxicities in humans. Special attention should also be paid to possible unwanted immune-system activation that can correlate with poor clinical outcome, such as M2-like macrophage activation. As demonstrated

by the addition of anti-PD-1, smart combinations of immunotherapeutic substances within the gel may provide an additional level of therapeutic potential, as well as an additional level of complexity. In summary, the reported data on the immunotherapeutic gel for post-cancer surgical treatment represent a promising approach that may contribute to better long-term control after resection in the future. □

Reinhard Liebers^{1,2,3*} and Dirk Jäger^{1,2,3*}

¹National Center for Tumor Diseases (NCT), Heidelberg, Germany. ²German Cancer Research Center (DKFZ), Heidelberg, Germany. ³Heidelberg University Hospital, Heidelberg, Germany. *e-mail: reinhard.liebers@nct-heidelberg.de; dirk.jaeger@med.uni-heidelberg.de

Published online: 10 December 2018
<https://doi.org/10.1038/s41565-018-0328-3>

References

1. Bianconi, E. et al. *Ann. Hum. Biol.* **40**, 463–471 (2013).
2. Clancy, S. *Nat. Educ.* **1**, 103 (2008).
3. Chen, Q. et al. *Nat. Nanotech.* <https://doi.org/10.1038/s41565-018-0319-4> (2018).

TOPOLOGICAL NANOPHOTONICS

Robust and compact waveguides

A nanofabricated twisted topological waveguide on silicon platform enables robust guiding of light at telecommunication wavelength.

Sabyasachi Barik and Mohammad Hafezi

One of the main challenges in nanophotonic systems is the presence of imperfections from fabrication processes that lead to losses and bleeding of photons while travelling in a waveguide. This can affect the output signal and stands true for photons of any frequency. Among ongoing attempts to tackle this problem, topological photonics^{1,2} is poised to provide an attractive solution because certain physical properties of these topological modes remain invariant under small perturbation of the system parameters, thus making them impervious to disorders. Now, writing in *Nature Nanotechnology*³, Shalaev et al. have used valley-Hall physics to explore the topological properties of photonic bandgaps in a photonic crystal waveguide. The researchers show a silicon nanophotonic crystal architecture that supports topological edge states as robust waveguide modes with high tolerance to structural disorders.

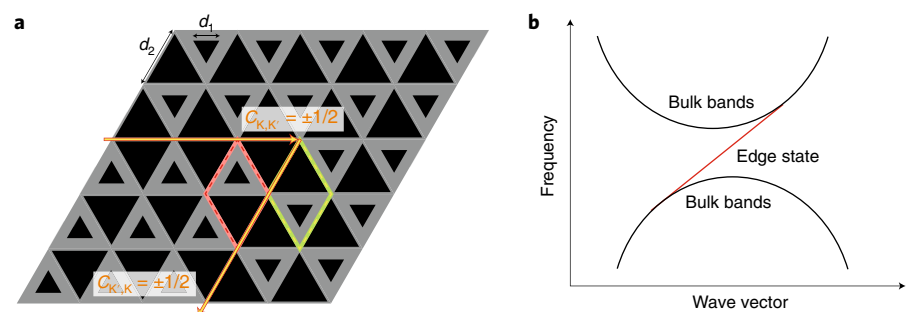


Fig. 1 | Valley-Hall topological waveguide. **a**, Schematic of the topological interface, which consists of two types of photonic crystal structures with different topological properties owing to opposite hole orientations, as shown in pink and green unit cells; d_1 and d_2 denote the lengths of the smaller and bigger triangles, respectively. The yellow/red arrow indicates the propagation of light around a sharp bend. **b**, The band diagram of such a device shows the presence of an edge state crossing the common bandgap region between the first and second bulk bands.

After an early demonstration of topological states in gyromagnetic materials for the microwave regime⁴, great

efforts have been made to realize similar states in the optical domain^{5,6}. Specifically, the built-in topological protection gives rise

to photonic edge states, with demonstrated quantitative robustness⁷. Moreover, in the field of semiconductor photonic crystal, implementation of non-trivial band topology has led to robust photon routing on a GaAs platform operating at a 900-nm wavelength⁸. Even though valley-Hall physics has been studied in a system of waveguide arrays⁹, demonstration of their topological properties had remained elusive. The work of Shalaev et al. fills this gap by demonstrating robust topological protection in a valley photonic crystal waveguide at telecommunication wavelength (1.55 μm). Remarkably, they manage to fabricate a small-footprint topological insulator using conventional nanofabrication techniques (electron beam lithography and etching) in a silicon-on-insulator platform. They measure the robustness of the topological waveguides by comparing light transmission through a straight and a twisted path. This photonic crystal design provides low-loss propagation and reduction of out-of-plane scattering of light.

A photonic crystal lattice with C_6 symmetry and equally sized triangular holes ($d_1 = d_2$) yields Dirac cones at K and K' points in the band structure for the transverse electromagnetic modes, whereas unmatched holes ($d_1 \neq d_2$) result in a C_3 symmetric photonic crystal which gives rise to bandgaps at the K and K' valleys (Fig. 1a). Shalaev et al. use triangular

holes in contrast to the traditional circular holes for their photonic crystal geometry to obtain a complete bandgap. This structure has a non-zero Berry curvature at each valley that can be calculated from the analytical description of the system Hamiltonian. The valley Chern number for each valley is $C_{K,K'} = \pm\frac{1}{2}$.

To realize the valley-Hall effect, Shalaev et al. create an interface between two structures with different orientations of a bigger triangle (Fig. 1a). Because the valley Chern number $C_{K,K'}$ changes its sign for these two geometries, their difference across the interface is 1. This determines the number of edge states for each valley, which is manifested by an edge state in the band structure (Fig. 1b).

The researchers study three different structures: (1) one with no change in orientation across the interface; (2) one with a straight interface; and (3) one with a trapezoidally shaped interface. By comparing transmissions of a broadband light source across these interfaces, the researchers found similar spectral dependence for both the linear and twisted waveguides, which agrees with their numerical results. This confirms suppression of reflection from sharp turns and robust topological transport.

However, owing to the time-reversal symmetry, there always exists a second edge state with opposite group velocity and helicity. As a result, these states are

not immune to disorders that can flip the helicities. Moreover, the effects of other types of defects, such as imperfect sizes or placement of holes, on these valley-protected edge states, and the robustness of different types of bends, still need to be evaluated. Nevertheless, the small footprint and on-chip fabrication technology reported by Shalaev et al. is likely to affect nanophotonic device fabrication for optical telecommunication and on-chip information processing. For example, one can think of making photonic structures at the nanoscale with low losses that can counteract the inevitable scattering of photons due to design and fabrication defects. \square

Sabyasachi Barik and Mohammad Hafezi*

University of Maryland, College Park, MD, USA.

*e-mail: hafezi@umd.edu

Published online: 12 November 2018

<https://doi.org/10.1038/s41565-018-0314-9>

References

1. Lu, L. et al. *Nat. Photonics* **8**, 821–829 (2014).
2. Ozawa, T. et al. Preprint at <https://arxiv.org/abs/1802.04173> (2018).
3. Shalaev, M. L., Walasik, W., Tsukernik, A., Xu, Y. & Litchinitser, N. M. *Nat. Nanotech.* <https://doi.org/10.1038/s41565-018-0297-6> (2018).
4. Wang, Z. et al. *Nature* **461**, 772–775 (2009).
5. Rechtsman, M. C. et al. *Nature* **496**, 196–200 (2013).
6. Hafezi, M. et al. *Nat. Photonics* **7**, 1001–1005 (2013).
7. Mittal, S. et al. *Phys. Rev. Lett.* **113**, 087403 (2014).
8. Barik, S. et al. *Science* **359**, 666–668 (2018).
9. Noh, J. et al. *Phys. Rev. Lett.* **120**, 063902 (2018).

SPINTRONICS

Heat-assisted microwave amplifier

In a magnetic tunnel junction, Joule heat increases the voltage-controlled magnetic anisotropy effect in the free layer and thereby pushes the amplification gain for microwaves beyond one.

Qiming Shao and Kang L. Wang

A magnetic tunnel junction (MTJ) consists of one tunnel oxide sandwiched between two magnetic layers: a free layer, whose magnetization is easy to manipulate, and a layer with fixed magnetization (Fig. 1a). The relative magnetization orientation — that is, the angle θ between the magnetization directions of these two layers — determines the tunnel resistance (Fig. 1b): if their magnetization is parallel, the MTJ is in a low-resistance state; if they are antiparallel, the MTJ has a high resistance. This change

in resistance determines the tunnel magnetoresistance ratio. The discovery of electric current-driven spin-transfer torques (STTs) enabled efficient manipulation of the free layer's magnetization without the need for an external magnetic field. This inspired various spintronic applications beyond magnetic random-access memories¹, including microwave generators and detectors. Writing in *Nature Nanotechnology*, Minori Goto et al. now demonstrate an MTJ-based spintronic microwave amplifier², which was originally proposed in 1997³.

MTJ-based microwave applications rely on the nonlinear dependence of the MTJ resistance on the relative magnetization angle. When the magnetization of the free layer precesses around the equilibrium position, the MTJ resistance also oscillates (Fig. 1b). For a microwave generator⁴ (Fig. 1c), a direct current is injected into the MTJ. The induced STT produces an auto-oscillation of the magnetization and thus an alternating MTJ resistance. The output voltage (V_{out}) is then the product of the direct current and the time-dependent